

We are IntechOpen, the world's leading publisher of Open Access books Built by scientists, for scientists

4,800

Open access books available

122,000

International authors and editors

135M

Downloads

Our authors are among the

154

Countries delivered to

TOP 1%

most cited scientists

12.2%

Contributors from top 500 universities



WEB OF SCIENCE™

Selection of our books indexed in the Book Citation Index
in Web of Science™ Core Collection (BKCI)

Interested in publishing with us?
Contact book.department@intechopen.com

Numbers displayed above are based on latest data collected.
For more information visit www.intechopen.com



Radiation Pattern Synthesis of Planar Arrays Using Parasitic Patches Fed by a Small Number of Active Elements

Jafar Ramadhan Mohammed and Karam Mudhafar Younus

Abstract

In this chapter, several planar array designs based on the use of a small number of the active elements located at the center of the planar array surrounded by another number of the uniformly distributed parasitic elements are investigated. The parasitic elements are used to modify the radiation pattern of the central active elements. The overall radiation pattern of the resulting planar array with a small number of active elements is found to be comparable to that of the fully active array elements with a smaller sidelobe level (SLL) at the cost of a relatively wider beamwidth and lower directivity. Nevertheless, the uses of only a small number of the active elements provide a very simple feeding network that reduces the cost and the complexity of the array. Simulation results which have been computed using computer simulation technology-microwave studio (CST-MWS) show that the sidelobe level of the designed array pattern with parasitic elements is considerably better than that of the similar fully active array elements. The proposed array can be effectively and efficiently used in the applications that require wider antenna beams.

Keywords: planar arrays, parasitic elements, driven elements, mutual coupling, feeding network, array pattern synthesis

1. Introduction

By properly controlling the design parameters of the antenna arrays, it is possible to generate the desired radiation characteristics such as higher directivity and lower sidelobe level. The most design parameters that have been given an increased attention for many practical applications are the amplitude and the phase excitations of the individual elements [1–3] in addition to the element's spacing [4, 5]. However, the practical implementation of the feeding networks in such arrays is known to be very complex and expensive.

Recently, the feeding networks were made very easy and practically efficient by controlling only a certain number of the active elements rather than all of the array elements [6, 7]. Other methods used a number of parasitic elements illuminated by a single active element to simplify the complexity issue of the feeding network.

These methods are of special interest because they are capable of introducing extra degrees of freedom that could effectively contribute to synthesize the desired array patterns without making any modification in the feeding networks of the active elements [8, 9]. Particularly, in [8], a planar array of complete parasitic dipoles which was placed under a single active $\lambda/2$ -dipole element to modify its radiation pattern was studied, while in [9], the authors considered a circular array of parasitic dipoles centered by one active dipole. The desired pattern was obtained by properly changing the spacing between the parasitic elements and the length of the parasitic elements, while the position and length of the driven element were kept fixed.

This chapter presents a new method for array pattern configuration with a low sidelobe level. The element type of the considered planar array is designed to be in the form of a simple rectangular patch. The feeding points of the active patches are optimally chosen such that the value of the VSWR becomes minimum. Moreover, the location of the feeding point has been obtained by the use of an optimization algorithm supported by the CST-MWS. In the proposed array, the elements are divided into two sub-arrays. The elements of the first sub-array which are located on the center of the planar array is referred as an active array, which contains only a small number of the array elements (usually one active element for an array of 3×3 elements and four active elements for other array sizes), whereas the second array subset contains the majority of the array elements which are parasitic, and their distances from the active ones need to be carefully chosen. Moreover, the second array subset may be selected either as a single or multiple rectangular rings according to the design requirements. The CST software is used to choose the most effective distances between the active and the parasitic elements (i.e., the most appropriate perimeter of the outer rectangular ring) such that the greatest reduction in the sidelobe level could be obtained with a smaller scarifies in the directivity.

2. Problem formulation

In order to highlight the major contribution of the proposed work, first we plot the radiation pattern of the fully active planar array elements that are designed with nonuniform amplitude excitation according to the Dolph polynomial to get the desired sidelobe level. For comparison, the uniformly excited planar array with 6×6 active elements is also included. **Figure 1** shows the radiation patterns of the Dolph excited planar array with SLL = -40 dBi and the uniformly excited planar

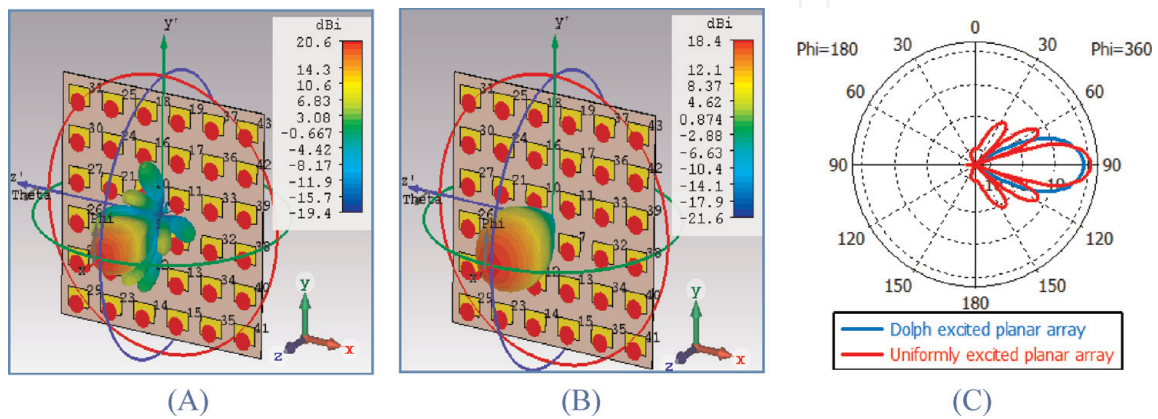


Figure 1. Results for 6×6 fully active array elements: (A) uniformly excited planar array; (B) Dolph excited planar array with SLL = -40 dBi; (C) radiation patterns in polar plots.

Fully active elements with Dolph excitations						Proposed array with parasitic elements				
Element	Amplitude	Phase	SLL (dB)	HPBW	Directivity (dB)	Amplitude	Phase	SLL (dB)	HPBW	Directivity (dB)
$\pm(1.1)$	0.0402	0	-21.4	23.1	18.4	0	0	-18.7	33.6	14.8
$\pm(1.2)$	0.1240	0				0	0			
$\pm(1.3)$	0.2004	0				0	0			
$\pm(2.1)$	0.1240	0				0	0			
$\pm(2.2)$	0.4675	0				0	0			
$\pm(2.3)$	0.6184	0				0	0			
$\pm(3.1)$	0.2004	0				0	0			
$\pm(3.2)$	0.6184	0				0	0			
$\pm(3.3)$	1.0000	0				1	0			
$\pm(4.1)$	0.2004	0				0	0			
$\pm(4.2)$	0.6184	0				0	0			
$\pm(4.3)$	1.0000	0				1	0			
$\pm(5.1)$	0.1240	0				0	0			
$\pm(5.2)$	0.4675	0				0	0			
$\pm(5.3)$	0.6837	0				0	0			
$\pm(6.1)$	0.0874	0				0	0			
$\pm(6.2)$	0.2021	0				0	0			
$\pm(6.3)$	0.2956	0				0	0			

Table 1.
The amplitude excitations of the Dolph and the proposed arrays.

array. In this figure, both array sizes are chosen to be 6×6 active elements, and the separation distance between any two successive elements in X- or Y-axis is chosen to be $\lambda/2$. **Table 1** shows the corresponding element excitations for the nonuniformly Dolph-distributed array.

From **Figure 1**, it can be seen that the Dolph excited array has a pattern with wider beamwidth and lower directivity than that of the uniformly excited planar array. More important, it can be seen that the Dolph excited array needs to be designed with a very precise values of the amplitude excitations to get the desired sidelobe pattern. Any simple variations from those computed values will lead to significant changes in the corresponding radiation pattern. In practice, the main reason for such variations in the amplitude excitations is due to the use of digital attenuators which are associated with the quantization errors due to the limited number of the quantized levels. Thus, the actual patterns are usually different from the desired ones.

In order to solve such an important problem in practice, the authors suggest an alternative method for obtaining the desired radiation pattern that does not need any digital RF components for amplitude scaling. In the proposed array, the magnitude excitations of the central active elements are assigned to the values of 1, while the parasitic elements are assigned to the values of 0. As the number of the active elements in the proposed array is chosen to be small, the value of the obtained gain is expected to be lower than that of the fully active array elements.

Moreover, the effect of the scattering, the mutual coupling, and the element type is all considered with the proposed array. Thus, the desired and the actual patterns are both expected to be in a good agreement.

Figure 2 shows the results of applying the proposed method under the use of only 4 active elements out of 36 elements (i.e., the number of the parasitic elements is 32). As can be seen, the proposed method with only four active elements is still capable to provide an acceptable radiation pattern as compared to that array of fully active elements.

As mentioned, the corresponding amplitude excitations of all of the abovementioned arrays are shown in **Table 1**.

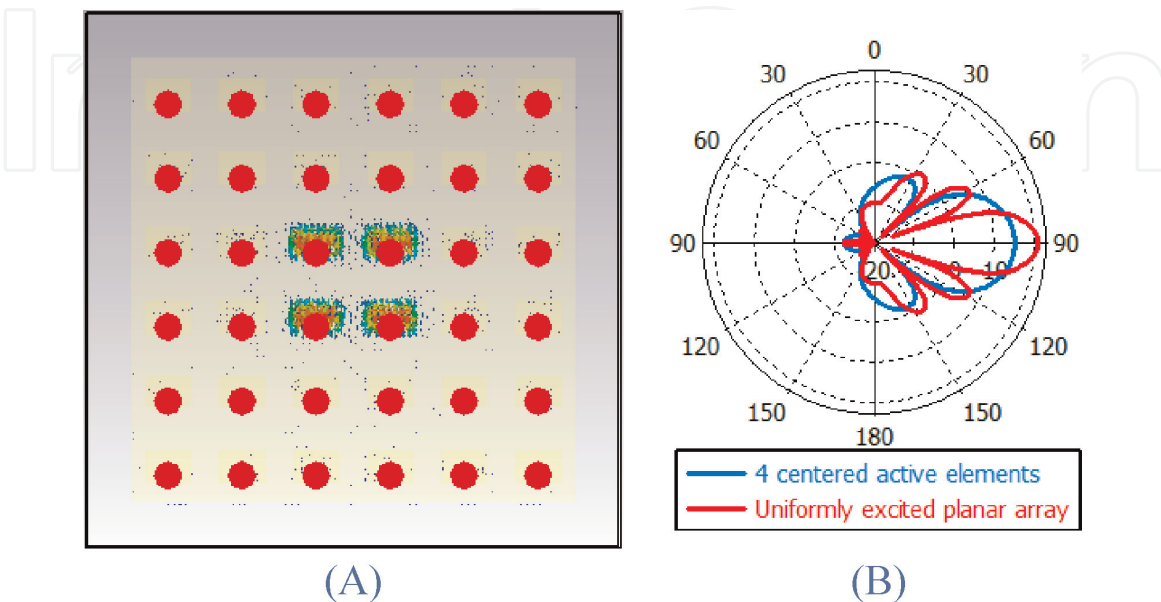


Figure 2. Results for the proposed planar array with 4 centered active elements and 32 parasitic elements; (A) current distribution and (B) radiation patterns in polar plots.

3. Description of the designed array

In this section, the procedures of designing a single patch element are presented; then it is straight forwarded to construct a required two-dimensional planar array. Generally, there are three methods in the design of a single microstrip patch: the transmission line model, cavity model, and full-wave model [1]. Among them, the transmission line model is considered in this work. This is mainly due to its simplicity and popularity. First, the patch dimensions (width and length) are designed according to the following:

$$\text{Width} = \frac{1}{2 f_r \sqrt{\mu_0 \epsilon_0}} \sqrt{\frac{2}{\epsilon_r + 1}} = \frac{v_0}{2 f_r} \sqrt{\frac{2}{\epsilon_r + 1}} \quad (1)$$

where v_0 is the velocity of the electromagnetic wave in the dielectric and f_r is the resonant frequency. On the other hand, the patch length usually seems to be electrically greater than its physical dimension due to the fringing effects. Consequently, the effective length (L_{eff}), effective dielectric constant (ϵ_{eff}), and the length extension (ΔL) have been computed as given by

$$\epsilon_{\text{eff}} = \frac{\epsilon_r + 1}{2} + \frac{\epsilon_r - 1}{2} \left[1 + \frac{12h}{\text{WP}} \right]^{-1/2} \quad (2)$$

$$L_{\text{eff}} = \frac{c}{2 f_r \sqrt{\epsilon_{\text{eff}}}} \quad (3)$$

$$\Delta L = 0.412h \frac{(\epsilon_{\text{eff}} + 0.3) \left[\frac{\text{WP}}{h} + 0.264 \right]}{(\epsilon_{\text{eff}} - 0.258) \left[\frac{\text{WP}}{h} + 0.813 \right]} \quad (4)$$

Then, the accurate length value of the patch is computed from

$$\text{Length} = L_{\text{eff}} - 2\Delta L = \frac{c}{2 f_r \sqrt{\epsilon_{\text{eff}}}} - 2\Delta L \quad (5)$$

Figure 3 shows a single patch element.

Note that, in this work, the coaxial probe is used to feed the single patch element. It is designed such that the value of reflection coefficient (S_{11}) is minimized at selected frequency value 2.4 GHz as shown in **Figure 4**.

Finally, to get the required planar array, a number of the designed patches are uniformly distributed along the X- and Y-axis. The radiation pattern of such array is then obtained by the vector addition of the radiation pattern of each individual

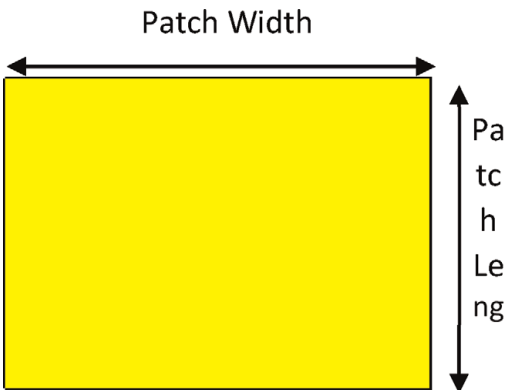


Figure 3.
Single patch element.

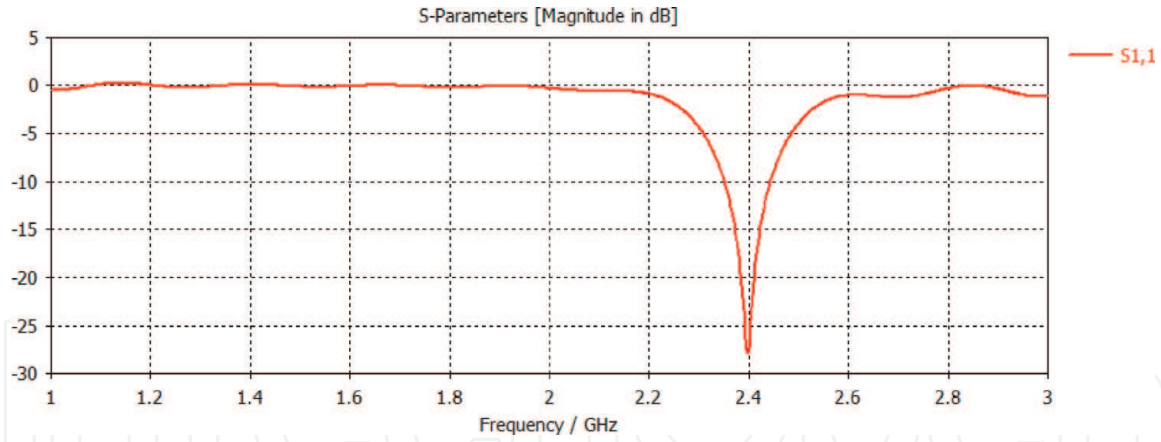


Figure 4.
Reflection coefficient (S_{11}) of the proposed patch antenna.

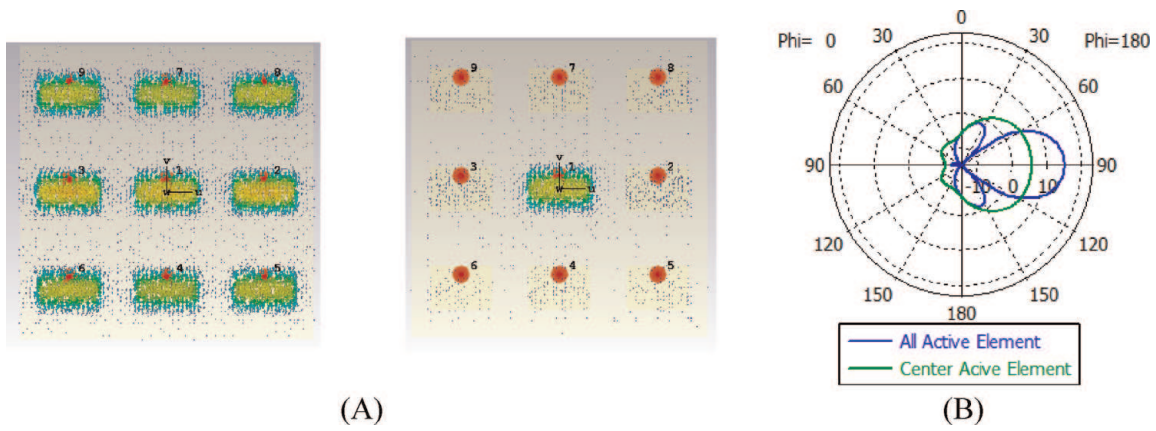


Figure 5.
Results for 3×3 planar arrays: (A) current distributions on both active and parasitic elements and (B) radiation patterns in the polar plot.

patch, taking into account the effect of mutual coupling between the array elements and the scattering effect.

4. Simulation results

To illustrate the effectiveness of the proposed method, different array configurations have been considered. In all examples, a rectangular planar array has been considered with $(N \times M)$ elements distributed on the XY-plane. The operating wavelength is chosen to be $\lambda = 125$ mm, and the separation distance between any two adjacent patches in both X- and Y-axis is $d = \lambda/2 = 62.5$ mm. The target angle is assumed to be at $(\theta, \varphi) = 0^\circ$.

In the first example, an array with 3×3 elements has been considered, and only the center element is chosen to be active, while the others are set to be parasitic.

Figure 5 shows the current distributions on the active and parasitic elements for both the fully active elements and the proposed array with only a single active element at the center of the array. For the fully active elements, the directivity (D) was 14.85 dBi, the sidelobe level was -16.69 dBi, and the half-power beamwidth (HPBW) was 33.6° , whereas for the proposed array these values were found to be $D = 5.41$ dBi, $SLL = -13.22$ dBi, and $HPBW = 97.30^\circ$.

In the second example, a planar array with 4×4 elements has been considered, and the separation distances between any two elements on the X- and Y-axis was set

to $\lambda/2$. Here, for the proposed array, only four centered elements are chosen to be active, while the other elements which are located on the perimeter of the array are chosen to be parasitic.

Figure 6 shows the results of the fully active array elements and the proposed array with only four active elements. For the former array, with all its elements being active, the D was 17.1 dBi, SLL was -14.4 dBi, and HPBW was 25.5° , while for the latter array with only four active elements, the D was 11.2 dBi, the SLL was -28.5 dBi, and the HPBW was 49.8° .

In the next example, an array with 5×5 elements is considered. For the proposed array, the elements that were located on the inner rectangular ring are chosen to be active (i.e., a number of eight elements), while the remaining elements are chosen to be parasitic as shown in **Figure 7**. For fully active array elements, the $D = 19.1$ dBi, $SLL = -13.9$ dBi, and $HPBW = 20.3^\circ$, while the values for the proposed array are found to be $D = 14$ dBi, $SLL = -13.9$ dBi, and $HPBW = 31.5^\circ$.

In all of the aforementioned examples, although the gain of the proposed array is relatively smaller than that of the fully active array elements, the radiation patterns are still in an acceptable shape. Moreover, these radiation patterns are produced with a very simple feeding network. Furthermore, the peak of the first sidelobe was significantly reduced down compared to that of the fully active array elements.

Finally, the performance of the proposed array with four active elements on the center of an array with size 6×6 elements is considered. The performance in terms

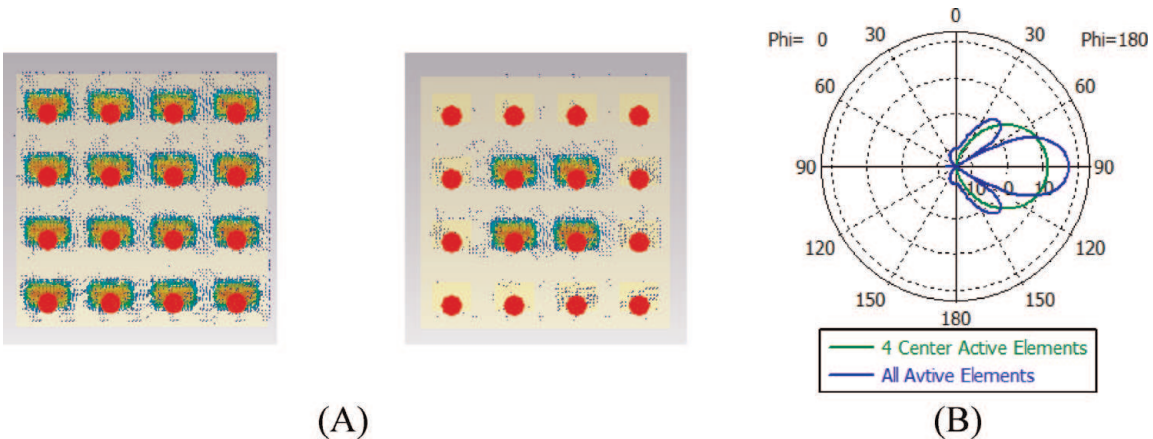


Figure 6.
Results for 4×4 planar arrays: (A) current distributions on both active and parasitic elements and (B) radiation patterns in the polar plot.

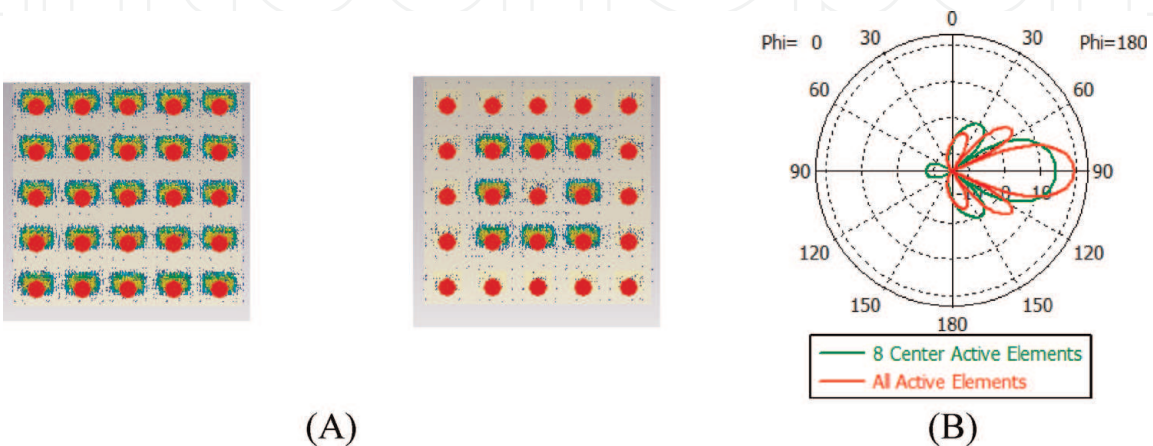


Figure 7.
Results for 5×5 planar arrays: (A) current distributions on both active and parasitic elements and (B) radiation patterns in the polar plot.

Spacing in (mm)	Spacing in (λ)	Directivity (dBi)	SLL (dBi)	HPBW ($^{\circ}$)
43.75	$0.35 \times \lambda$	10.60	-26.05	54.5
56.25	$0.45 \times \lambda$	11.21	-35.80	50.9
62.50	$0.50 \times \lambda$	11.30	-37.60	50.4
68.75	$0.55 \times \lambda$	11.30	-33.95	50.6
81.25	$0.65 \times \lambda$	11.32	-30.86	47.8
93.75	$0.75 \times \lambda$	11.60	-34.20	46.6

Table 2.
The performance of the proposed array versus separation distances between active and parasitic elements.

of D, SLL, and HPBW is investigated under various values of the separation distances between the active and the parasitic elements as shown in **Table 2**.

5. Conclusions

Various planar array configurations are designed to produce radiation patterns with various characteristics, such as various beamwidth and low sidelobe level. It is shown that the radiation pattern of a small number of the active elements can be improved by properly selecting the most efficient configuration of the parasitic elements which are usually chosen from the outer elements of the array. Unlike the existing array pattern synthesis methods which usually use the digital phase shifters and/or attenuators, the proposed method needs only switches to turn the array elements either on (active) or off (parasitic). Therefore, it is robust to the excitation errors and simpler and cheaper to implement. However, when some elements of the array are switched off, then the obtained gain will be reduced.

Author details

Jafar Ramadhan Mohammed* and Karam Mudhafar Younus
College of Electronics Engineering, Ninevah University, Mosul, Iraq

*Address all correspondence to: jafarram@yahoo.com

IntechOpen

© 2019 The Author(s). Licensee IntechOpen. This chapter is distributed under the terms of the Creative Commons Attribution License (<http://creativecommons.org/licenses/by/3.0>), which permits unrestricted use, distribution, and reproduction in any medium, provided the original work is properly cited.



References

- [1] Balanis CA. Antenna Theory, Analysis and Design. 4th ed. Hoboken, New Jersey: Wiley; 2016
- [2] Mailloux RJ. Phased Array Antenna Handbook. 2nd ed. Norwood, MA: Artech House; 2005
- [3] Haupt RL. Antenna Arrays: A Computational Approach. Hoboken, New Jersey: John Wiley and Sons; 2010
- [4] Mohammed JR. Thinning a subset of selected elements for null steering using binary genetic algorithm. Progress in Electromagnetics Research. 2018;**67**: 147-157
- [5] Ismail TH, Dawoud MM. Null steering in phased arrays by controlling the element positions. IEEE Transactions on Antennas and Propagation. 1991;**39**:1561-1566
- [6] Mohammed JR. Optimal null steering method in uniformly excited equally spaced linear arrays by optimizing two edge elements. Electronics Letters. 2017; **53**(13):835-837
- [7] Mohammed JR. Element selection for optimized multi-wide nulls in almost uniformly excited arrays. IEEE Antennas and Wireless Propagation Letters. 2018;**17**(4):629-632
- [8] Rodriguez-Gonzalez JA, Ares-Pena F. Design of planar arrays composed by an active dipole above a ground plane with parasitic elements. Progress in Electromagnetics Research. 2011;**119**: 265-277
- [9] Hemant P, Gautam KM. Design of non-uniformly spaced circular arrays of parasitic dipoles for lower side lobe level with maximum directivity. Advanced Electromagnetics. 2018;**7**(1):51-56